RAPID RAC GTP-ASE ACTIVATION IN LIVE CELLS BY MECHANICAL STRESS IS INDEPENDENT OF SRC

BY

YEH CHUIN POH

THESIS

Submitted in partial fulfillment of the requirements
for the degree of Master of Science in Mechanical Engineering
in the Graduate College of the
University of Illinois at Urbana-Champaign, 2009

Urbana, Illinois

Advisor:

Professor Ning Wang

ABSTRACT

It is well-known that mechanical forces are crucial in regulating functions of every tissue and organ in a human body. However, it remains unclear how mechanical forces are transduced into biochemical activities and biological responses at the cellular and molecular level. Using the magnetic twisting cytometry technique, we applied local mechanical stresses to living human airway smooth muscle cells with a magnetic bead bound to the cell surface via transmembrane adhesion molecule integrins. The temporal and spatial activation of Rac, a small guanosine triphosphatase, was quantified using a fluorescent resonance energy transfer (FRET) method that measures changes in Rac activity in response to mechanical stresses by quantifying intensity ratios of ECFP (enhanced cyan fluorescent protein as a donor) and YPet (a variant yellow fluorescent protein as an acceptor) of the Rac biosensor. The applied stress induced rapid activation (less than 300 ms) of Rac at the cell periphery. In contrast, platelet derived growth factor (PDGF) induced Rac activation at a much later time (>30 sec). It is known that PDGF-induced Rac activation depends on Src activity. There was no stress-induced Rac activation when a mutant form of the Rac biosensor (RacN17) was transfected or when the magnetic bead was coated with transferrin or with poly-L-lysine. Surprisingly, pre-treatment of the cells with specific Src inhibitor PP1 or knocking-out Src gene had no effects on stress-induced Rac activation. In addition, eliminating lipid rafts through extraction of cholesterol from the plasma membrane did not prevent stress-induced Rac activation, suggesting a raft-independent mechanism in governing the Rac activation upon mechanical stimulation. Further evidence indicates that Rac activation by stress

depends on the magnitudes of the applied stress and cytoskeletal integrity. Our results suggest that Rac activation by mechanical forces is rapid, direct and does not depend on Src activation. These findings suggest that signaling pathways of mechanical forces might be fundamentally different from those of growth factors.

Note: The results contained within this manuscript have been published in the scientific journal *PLoS ONE* under the title "Rapid Actication of Rac GTPase in Living Cells by Force Is Independent of Src".

To my dear Father and Mother

Boon Sing Poh
Good Cam Ng

and my beloved brothers

Yeh Han Poh
Yeh Tze Poh
Yeh Ern Poh

for their love and continuous support.

ACKNOWLEDGEMENTS

First and foremost, I would like to thank my research advisor, Professor Ning Wang for introducing me to the field of cell mechanics and his guidance throughout this project. Next, I would like to extend my gratitude to the people in my research group: Dr. Sungsoo Na, Farhan Chowdhury, Arash Tajik, and Russell Borduin. These people have provided support and invaluable advice throughout this project. They have helped me in my understanding of mechanobiology and have been a great encouragement during this steep learning process. I would also like to thank Myung Eun Shin and Steven Chang for helping me in the amplification of biosensors. Heartfelt thanks to Richard Wang for initiating this project and for collecting and analyzing some early experimental results. Dr. R. Panettieri of the University of Pennsylvania is thanked for providing the Human Airway Smooth Muscle (HASM) cells. Finally, I would like to express my appreciation to Dr. Mingxing Ouyang and Dr. Yingxiao Wang from the Bioengineering Department at the University of Illinois for the gift of Rac1 biosensor.

TABLE OF CONTENTS

LIST OF FIGURES

CHAPTER 1

INTRODUCTION

1.1 Mechanotransduction

Mechanotransduction is the process by which living cells sense mechanical stimuli and convert them into intracellular biochemical signals that elicit physiological or pathological responses. It has been established that mechanical forces play vital roles in shaping the normal functions of all tissues and organs of human beings [1]. The mechanical environment of cells crucially influences many cell functions [2]. However, it remains largely mysterious how mechanical stimuli affect tissue and organ functions. Specifically, it is not clear how mechanical forces are transmitted into biochemical signals inside the living cells; i.e., the mechanism of mechanotransduction. It is of great importance to understand how cells sense and adapt to mechanical stresses because cell shape, cell behavior and cytoskeletal structure are influenced by the mechanical environment the cells are in [1, 3]. These mechanical stresses can be generated by cell-cell interaction through E-cadherin molecules, by pressure generated in vessel walls, by shear stress due to blood flow, or by the cell exerting on the extracellular matrix (ECM) adhesions through the contractility of the cytoskeletal known as tractional forces [4, 5]. Over the years, it has been clearly demonstrated that in determining cell morphology, transcriptional programs, and cell fate, the stiffness of a cell's substrate and cell traction forces provide as much input as do chemical messengers [6 , 7] It has also been shown that several molecules and cellular structures are involved in mechanotransduction. For example, stress activated ion channels, transmembrane proteins that mediate cell-matrix

or cell-cell contacts, focal adhesion complexes, membrane lipids, glycocalyx proteins, and also G-protein coupled receptors can serve as mechanosensors and transducers [1].

1.2 Models for Mechanotransduction

Over the years, several models of mechanotransduction have been proposed such as stretch-activated membrane ion channel opening and local plasma membrane protein unfolding [8]. The main thrust of these models is that mechanotransduction, similar to the soluble factor induced signal transduction, initiates at the cell membrane by inducing local conformational changes or unfolding of membrane-bound proteins at the site of a local force followed by a cascade of passive diffusion or active translocation processes for downstream signaling. This is consistent with the theory of the classical continuum mechanics of St. Venant's principle that a local force must cause only a local deformation. Different features of mechanotransduction have been shown in recent years, including myosin dependent substrate rigidity feedback [7, 9], myosin dependent lamellipodial contractions [10], selective recruitment of adaptor proteins by flow induced shear stress [11], stress induced alterations of focal adhesion zyxin proteins dissociation constant [12], force induced structural adaptation at focal adhesions [13], and mechanical adaptation at focal adhesions [3] or in the whole cell [14]. It was also shown that substrate stiffness strongly influences stem cell differentiation [9].

1.3 Function of Src and Rac Proteins

Src is a family of proto-oncogenic tyrosine kinases. Src kinase plays crucial roles in a variety of cellular functions, including angiogenesis and cancer development [15]. It has been shown that angiogenic VEGF activates Src to regulate cell motility and migration during angiogenesis [16]. Src is also known to regulate the integrin-cytoskeleton interaction [17], which is essential for the transduction of mechanical stimuli [18; 19; 20]. Src binds constitutively and selectively to β3 integrins through an interaction involving the c-Src SH3 domain and the carboxyl-terminal region of the β3 cytoplasmic tail. Clustering of integrins activates Src and induces phosphorylation of Syk, a c-Src substrate [21]. It has been reported that Src contributes to cell migration by modulating Rac [22].

Rac is a subfamily of the Rho-family of GTPases, small (~21 kDa) signaling G proteins which function as molecular switches in a number of different signaling cascades. Rac GTPase is a regulator of many cellular processes, including cell cycle, cell-cell adhesion, and cell protrusion and lamellipodia formation [22]. Activation of Rac occurs when the exchange of guanosine diphosphate (GDP) for guanosine triphosphate (GTP) occurs. This G protein is regulated by two classes of proteins, namely the guanine nucleotide exchange factor (GEF), and the GTPase-activating protein (GAP). GEF releases GDP from the G protein and replaces it with GTP, thus activating the protein to bind with its downstream effectors. GAP catalyses the hydrolysis of GTP to GDP bound to the G protein, therefore causing it to become inactive [23, 24]. The activation of Rac was inhibited when the cell was transfected with a dominant inhibitory mutant Rac protein, N17Rac1. A schematic of the Rac activation process is shown and described in

Fig. 2. The small GTP-binding protein Rac is concentrated at the cell periphery and has been shown to stimulate actin filament accumulation at the plasma membrane, forming membrane ruffles [24].

1.4 Hierarchical Relationship of Src and Rac

For soluble factor induced signal transduction, it has been shown that platelet derived growth factor (PDGF) activates Src kinase [25]. PDGF also induces a strong Rac activation at the membrane ruffles and a moderate overall activation of Rac in the whole cell [26]. However, PDGF-induced Rac activation is abolished by inhibition of Src through pretreatment of PP1, a specific Src inhibitor [26]. This indicates that Src is necessary for growth factor induced Rac activation. Activation of Src kinase in turn leads to activation of Rac. Src and Rac, however, mutually regulate each other in response to PDGF but differ in subcellular distribution. Rac is highly polarized and concentrates at the leading edge of the cell periphery, whereas Src is relatively uniform distributed [26].

1.5 Fluorescence Resonance Energy Transfer (FRET)

Fluorescence resonance energy transfer (FRET) is a mechanism that occurs between two different chromophores (the donor and the acceptor) with overlapping emission absorption spectra [27]. A chromophore is a part of a molecule that is responsible for its color. Light of a certain wave length that is incident on a chromophore can be absorbed by exciting an electron from its ground state into an excited state. The excited chromophore now emits a visible light of a different wave length. An acceptor

chromophore is now able to be excited by the emission light wave of the excited donor. A donor chromophore, in its electronic excited state transfers energy to an acceptor chromophore that is of close proximity (< 10 nm) through nonradiative dipole-dipole coupling. This mechanism of transferring energy from the donor to acceptor is termed FRET. An example of FRET mechanism between cyan florescent protein (CFP) and yellow fluorescent protein (YFP) is shown in Fig. 1. FRET-based imaging microscopy is commonly used as a sensitive probe of protein-protein interactions and protein conformational changes *in vivo* [27].

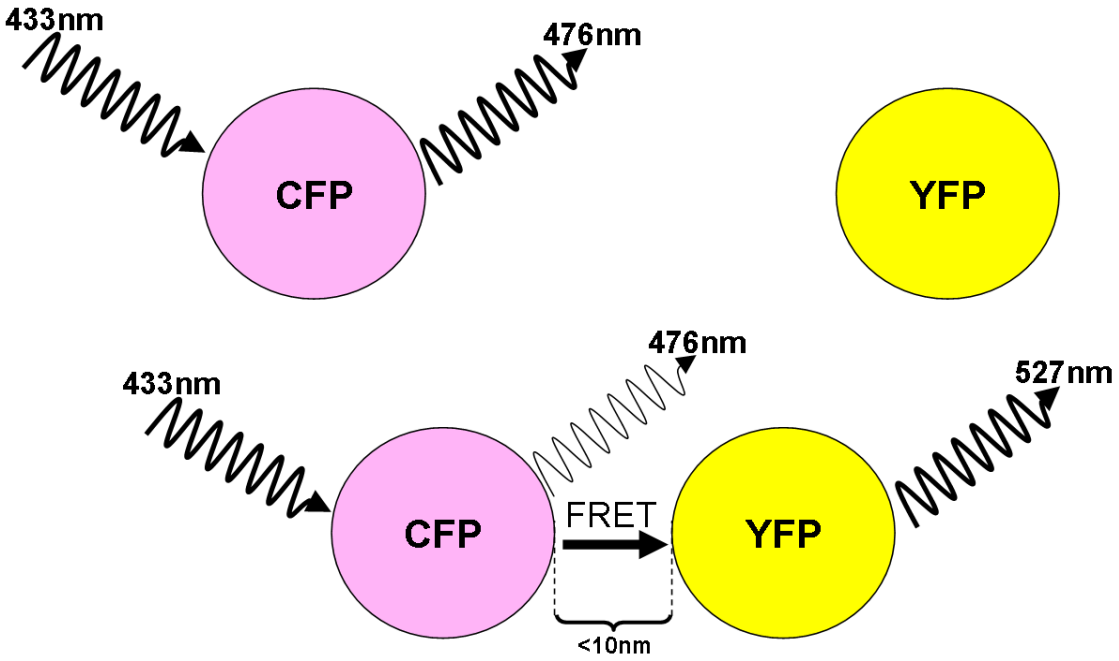

Figure 1. *Schematic of FRET mechanism. The donor CFP is excited with a light of wavelength 433nm and emits a light of wavelength 476nm. The fluorescence emission of CFP overlaps the excitation of YFP. When both CFP and YFP are within a proximity of <10nm, a large amount of energy transfer occurs from CFP to YFP, causing a significant decrease in CFP emission and an increase in YFP emission.*

1.6 Objective of Study

Though it has been shown that Src can be activated through mechanical stress application [28], it has yet to be shown whether Rac can also be activated through mechanical stress. If Rac activation by mechanical forces were similar to that by PDGF, one would expect the stress-induced Rac activation to be dependent also on Src activation. In sharp contrast, if Rac GTPase could be directly activated by mechanical forces at the cell surface, then its activation would not depend on Src activity. Therefore, the objectives of this study are as follows. First is to examine whether Rac can be directly activated by mechanical stress. Second, if Rac activation by stress is possible, is stress induced Rac activation independent of Src. Third, does stress induced Rac activation imitate the dominant mechanotransduction model, whereby mechanical force induces local activation of proteins [8].

CHAPTER 2

MATERIALS AND METHODS

2.1 Ethics Statement

Human airway smooth muscle (HASM) cells used were de-identified and supplied by Dr. Panettieri who obtained the tissue through NDRI (National Disease Research Interchange) in a manner that excludes all unique identifying information. There is no consent form sent with the tissue as per NDRI. All our procedures were approved by the Institutional Review Board of University of Illinois at Urbana-Champaign.

2.2 Cell Culture, Reagents and Transfection

Human airway smooth muscle (HASM) cells were isolated at autopsy within 8 hrs of death from tracheal muscle of lung transplant donors (approved by the University of Pennsylvania Committee on studies involving human beings) at University of Pennsylvania in Dr. Panettieri's laboratory [29]. A monoclonal antibody that recognizes only the α- and β-isoactin of smooth muscle was used to identify the cells as smooth muscle cells. Cells were cultured at a density of 10,000 cells/cm^2 in Ham/F12 media, supplemented with 10% fetal bovine serum, 2mM L-glutamine, 100 μg/ml of penicillin, 100 μg/ml of streptomycin, 12 mM NaOH, 1.7 μM $CaCl_2$, 50 μg/ml gentamicin, and 2.5 μg/ml amphotericin B. When cells reached passage two, they were shipped for further culturing and experiments. Cells at passage 3-8 were used for all experiments. These

cells still maintain smooth muscle cell morphology and physiological responsiveness to agonists at passage 8. After cells reached confluence in culture dishes, they were serum deprived for 24 h before being trypsinized. Following trypsinization, cells were plated in serum free medium (IT, i.e. Insulin-Transferrin containing medium) overnight in 35-mm dishes for experiments. HASM cells do not enter cell cycle but maintain contractile profile in IT medium. The Src/Yes/Fyn triple-knockout (SYF-/-) mouse embryonic fibroblast (MEF) cells were cultured and maintained in DMEM (Sigma) supplemented with 10% fetal bovine serum (HyClone), 100U/ml penicillin, 100μg/ml streptomycin, and 2mM L-Glutamine at 37^{o}C in 5% CO_2. The 35-mm dishes (No. 00, VWR) were pre-coated with collagen-1 (0.02 mg/ml) in phosphate-buffered saline (PBS) to facilitate absorption of protein onto the wells. Then the cells were plated in the wells at ~7,000 cells/well for live cell imaging. A Src-selective tyrosine kinase inhibitor, 4-Amino-5-(4-methylphenyl)-7-(t-butyl) parasol (3,4-d)-pyrimidine (PP1) from Biomol was used at final concentration of 10 μM for 1 hr. A specific inhibitor of Rac GTPase, N6-[2-[[4-(Diethylamino)-1-methylbutyl]amino]-6-methyl-4-pyrimidinyl]-2-methyl-4,6-quinolinediamine trihydrochloride (NSC23766), from Tocris Bioscience (Ellisville, Missouri), was used at final saturating concentration of 100 μM for 1 hr. Platelet-derived growth factor (PDGF) (Sigma; St. Louis, MO) was used at final saturating concentration of 10 ng/ml. Methyl-β-cyclodextrin (MβCD), was used at a concentration of 10 mM to extract cholesterol from the plasma membrane. All cytoskeletal inhibitors were purchased from Sigma.

2.3 Rac Biosensor

The Rac biosensor has been improved in its sensitivity by replacing the original fluorescence proteins with ECFP (as a donor for FRET) and YPet (as an acceptor for FRET) [26] (Fig. 2), based on a Rac biosensor pRaichu-Rac/RacCT, a gift from Dr. Michiyuki Matsuda at Kyoto University [30]. The probe of pRaichu-Rac/RacCT has been very well characterized in terms of its specificity [30]. The probes were transfected into HASM cells by adding 3 μg per 35-mm dish or SYF-/- MEF cells by adding 1 μg per 35-mm, both using Lipofectamine, following protocols provided by the manufacturer (Invitrogen) and incubated for 24 hours. A mutant Rac biosensor pc'-Rac(N17)-YPet was used as a negative control, where Thr^{17} of Rac1 was replaced by Asn, as previously described Itoh *et al* [30].

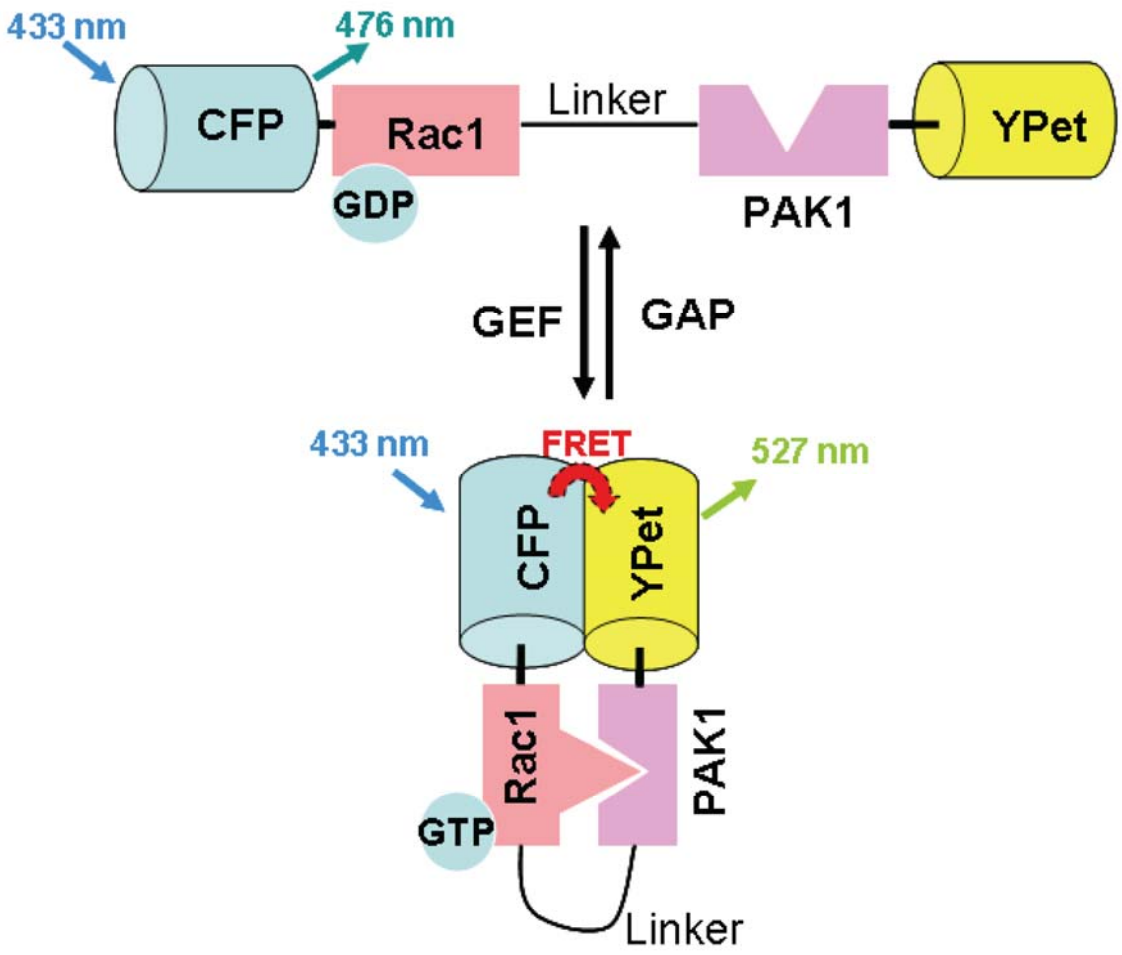

Figure 2. *Quantification of Rac activity in a living cell by FRET.* ***Top****, the Rac GTPase (Rac1) and its substrate PAK1 are connected by a flexible linker. Rac1 is associated with Cyan fluorescent protein (CFP) and its substrate PAK1 (p21-activated kinase 1) (a serine-threonine kinase activated by Rac GTPase) with YPet (a variant of yellow fluorescent protein). When Rac is not activated, excitation at 433 nm yields an emission of 476 nm via CFP, no FRET occurs.* ***Bottom****, when Rac is activated by GEF (guanine nucleotide exchange factor) that stimulates GTPases by catalyzing the exchange of guanosine diphosphate (GDP) for guanosine triphosphate (GTP), Rac1 proceeds with conformational changes so that it binds specifically with its substrate PAK1. The binding of Rac1 with PAK1 leads to close association of CFP with YPet. Excitation of CFP at 433 nm now yields an emission of 527 nm via YPet, FRET occurs. In the presence of GAP (guanosine triphosphatase (GTPase)-activating protein) that hydrolyses GTP to*

GDP, Rac1 dissociates from PAK1, the Rac biosensor returns to inactivated and extended form. (Modified from [30])

2.4 FRET Microscopy

A Leica inverted microscope was integrated with a magnetic twisting device and a Dual-View system (Optical Insights, Tucson, AZ) to simultaneously acquire both CFP and YFP emission images in response to stress. For emission ratio imaging, the Dual-View Micro-Imager (Optical Insights) was used. The CFP/YPet Dual EX/EM (FRET) (OI-04-SEX2) has the following filter sets: CFP: excitation, S430/25, emission S470/30; YPet: excitation, S500/20, emission S535/30. The emission filter set uses a 515 nm dichroic mirror to split the two emission images. Cells were illuminated with a 100W Hg lamp. For FRET imaging, each CFP (1344 pixels by 512 pixels) and each YPet image (1344 pixels by 512 pixels) were simultaneously captured on the same screen using a CCD camera (Hamamatsu C4742-95-12ERG) and a 40X 0.55NA air objective.

2.5 Optical Magnetic Twisting Cytometry

The magnetic twisting cytometry (MTC) is a device used to deliver small forces to specific sites on the cell membrane. Optical magnetic cell twisting is an extension of the magnetic cell twisting technique [31, 32] to any modes of forcing. Ferromagnetic beads (~4.5 μm diameter) were coated with saturated amount of Arg-Gly-Asp (RGD)-containing peptides, ligands for integrin receptors (the ligand density on the bead was measured to be about 1 RGD-peptide per 2 nm^2 of bead surface area). The beads were suspended in serum free medium, and ~20,000 beads were added to an individual cell well. The cells were incubated for 15 min to allow for binding of the beads to integrins on

the cell surface. Excess and unbounded beads were removed by washing with PBS before the dish of cells was placed under the microscope. Similar technique was used to coat the ferromagnetic beads with transferrin or poly-L-lysine, both at 50 μg/ml per mg bead. The binding specificity of bead binding was determined following protocols described previously [32]. The microscope stage was heated to maintain 37^0C for the cells in a dish. The magnetic moments of each batch of self-made ferromagnetic beads were calibrated according to published methods [32]. The technique of applying twisting torques to cells in a dish under a microscope had been described in detail [33]. The beads were magnetized by a strong (1,000 G) and short (<100 μs) magnetic field pulse oriented at the horizontal direction using the magnetizing coils. The twisting current was driven by a current source controlled by a computer. The magnetic twisting field can be varied from 0 to 75 Gauss (G). A step function field (i.e. constant magnetic field) of 5, 10, 25, or 50 Gauss (equivalent of 1.8, 3.6, 8.8 or 17.5 Pa stress) was applied. The stress applied to the cell {in Pascals (Pa) where 1 Pa equals to 1 picoNewton per micrometer square ($pN/\mu m^2$)} is defined as the ratio of the applied torque (in pN/μm) to six times the bead volume (μm^3). The applied stress (in Pa) can be obtained by multiplying the bead constant (in Pa/G) with the applied twisting field (in G). The bead constant is a magnetic property of the bead and differs from each batch. To calibrate and calculate the bead constant (in Pa/G), the magnetic beads can be immersed in a medium with known viscosity and a twisting field (in G) of variable magnitude is applied while measuring the angular velocity. Calibration procedure on converting applied magnetic field to applied stress on cell surface has been described by Valberg *et al* [34].

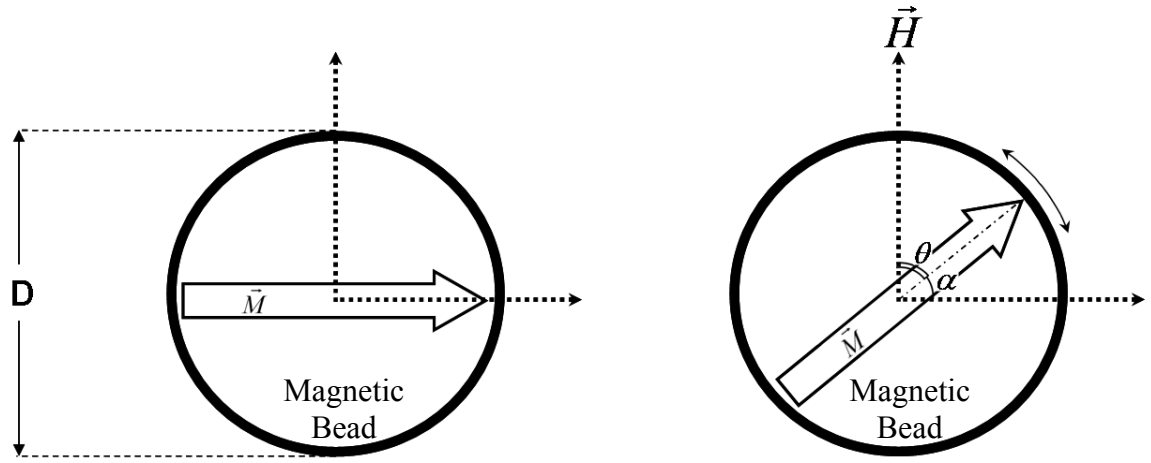

Figure 3. *Twisting of ferromagnetic bead.* ***Left,*** *an impulse application of a strong magnetic field (1000G for <100 μs) along the horizontal direction results in magnetization and alignment of the magnetic moment. D is the diameter of the magnetic bead while* $\vec{M}$ *is the magnetic moment.* ***Right,*** *application of a weaker magnetic field,* $\vec{H}$ *(0 to 75 G) in the direction perpendicular to the original field causes the magnetic bead to rotate or twist by an angle* α *. A free standing bead absent of external forces will rotate 90*^{o} *in to complete alignment with the twisting field. When the bead is bound to the cell via integrins, there is a resistance to deformation and the bead rotation becomes small.*

The equation for magnetic torque (T) as described by Valberg et al [34] is

$$T = \mu_o\left(\vec{M} \times \vec{H}\right) \tag{1}$$

where μ_o = magnetic permeability in vacuum = $4\pi \times 10^{-7}\, N/A^2$

$\vec{M}$ = bead magnetic moment

$\vec{H}$ = magnetic field

The magnetic permeability of a material is the degree of magnetization that it receives when it responds linearly to a magnetic field. It is expressed in the units of H/m (Henry per meter) or N/A^2 (Newton per ampere squared).

The cross product of the magnetic moment and the magnetic field yields the following torque equation.

$$T = \mu_o |M||H| \sin\theta \tag{2}$$

where θ is the small angle of the bead's magnetic moment, $\vec{M}$ relative to the twisting field, $\vec{H}$. $|M|$ and $|H|$ are the magnitudes of vectors $\vec{M}$ and $\vec{H}$. Equation 2 above can be simplified to

$$T = \mu_o MH \sin\left(\frac{\pi}{2} - \alpha\right) \tag{3}$$

$$T = \mu_o MH \cos\alpha \tag{4}$$

where α is the angle of deflection of the bead as shown in Fig. 3. The magnitude of the specific torque, T_{sp} expressed as torque, T per unit bead volume, V is described by

$$T_{sp} = \frac{T}{V} = \frac{\mu_o M}{V} H \cos\alpha \tag{5}$$

The specific torque which has units of pascal (Pa which is also N/m^2) is now defined as 1/6 of the average applied stress, σ as explained in the later part of this section. Therefore, the average applied stress, σ can be expressed as

$$\sigma = \frac{T_{sp}}{6} = \frac{T}{6V} = \frac{\mu_o M}{6V} H \cos\alpha \tag{6}$$

Since the bead constant is defined as $c = \frac{\mu_o M}{6V}$, the average applied stress, σ can be simplified to the following equation

$$\sigma = cH \cos\alpha \tag{7}$$

where $\frac{\pi}{2} - \alpha$ is the angle of bead's magnetic moment relative to twisting field, c is the bead constant (Pa/G), and H is the applied magnetic field (G). Throughout this study, we used beads with c = 0.35 Pa/G. Due to the fact that when beads are bound to the cell surface, the transmission of force to the cytoskeleton causes an increase of resistance to deformation [32], thereby reducing the bead rotation. When the angle of deflection of the bead is small, which is usually the case, $\cos\alpha \approx 1$. Equation 7 can therefore be approximated as

$$\sigma \approx cH \tag{8}$$

We can now easily calculate the average applied stress by multiplying the known bead constant, c with the applied magnetic field, H. From equation 5 above, it is shown that the applied torque, T is equal to the specific torque, T_{sp} multiplied by the bead volume, V and the physical definition of applied torque on a spherical bead is force, F times the diameter of the bead, D as seen in Fig. 4. Therefore, the equation describing the applied torque is

$$T = FD = T_{sp}V \tag{9}$$

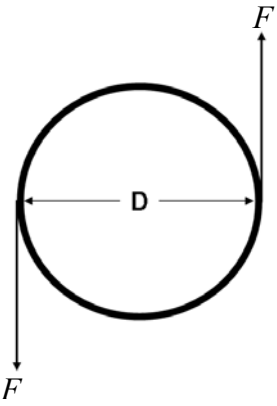

Figure 4. *Torque on a spherical bead. Torque is a moment force which is similar to a twist, where it describes the ability to produce torsion and rotation about an axis. Torque is calculated by taking the vector product of the radius vector from the axis of rotation to the point of force application and the force vector. In this case, the radius vector is* r *and the force vector is F. Since the coupled force acts on both sides of the bead in the same counter clockwise direction, the net torque is therefore the sum of torques produced by the coupled forces.* $T = 2(r \times F) = FD.$

Since force, F is equivalent to applied stress, σ multiplied by the bead area, $4\pi r^2$. The above equation can then be rearrange to yield applied stress, σ as a function of applied torque, T and volume, V.

$$T = (\sigma 4\pi r^2)D \tag{10}$$

$$\sigma = \frac{T}{(4\pi r^2)2r} \tag{11}$$

$$\sigma = \frac{T}{8\pi r^3} \tag{12}$$

$$\sigma = \frac{T}{8\frac{3}{4}\left(\frac{4}{3}\pi r^3\right)} \tag{13}$$

$$\sigma = \frac{T}{6V} \tag{14}$$

It is for this reason that we have defined applied stress, σ as one sixth of the specific torque, T_{sp}. Because the magnetic field is applied over the entire dish, only one biochemical activity assay may be performed per dish. A two-tailed Student's t-test was used for statistics.

2.6 Image Analysis

A customized Matlab (Mathworks) program was used to obtain YPet/CFP emission ratios of the Rac biosensor in living cells. The CFP and YPet images were first split in to its constituent image by cropping the original composite. CFP and YPet images at each time point were then background-subtracted and the YPet image was used to generate a binary mask based on an input threshold so that the pixel value inside the cell was set to 1 and the pixel value outside the cell was set to 0. The binary mask can be generated using a user defined intensity threshold or by using Matlab's "graythresh" function based on Otsu's method [35]. After multiplication of the original YPet image by the mask image, this updated YPet image and the CFP image were aligned pixel-by-pixel by maximizing the normalized cross-correlation coefficient of the CFP and YPet images [28]. Aligned YPet/CFP emission ratios were normalized to the lower emission ratio and displayed as a linear pseudocolor. Since Rac activation occurs only at the cell periphery, the signal to noise ratio was increased by obtaining the normalized YPet/CFP emission ratio at 2 μm annulus around the cell boundary. A binary mask of the cell with the inside

set to 1 was obtained by a separate customized Matlab program using the gray scale images with black background that was previously generated. The same image was then scaled down by 2 μm on all sides while maintaining the cell center of mass and image aspect ratio. A new binary mask was then obtained with the area outside of the cell set to 1. The original gray scale image was multiplied by the first and second binary masks yielding a 2-μm thick gray scale cell annulus image. The mean intensity of the gray scale cell annulus was then calculated as YPet/CFP emission ratio.

2.7 Experimental Protocols

HASM cells in passages 4-10 were used in all experiments. After HASM or SYF-/- MEF cells were plated on collagen-1 coated dishes overnight, the cells were transfected with CFP-YPet Rac biosensors for 24 hrs. The culture medium was then removed from the dish so that only the cells in the glass well region are submerged in medium. 30 to 40 μl of RGD-coated magnetic bead was attached to the cell apical surface for 15 min to allow for integrin clustering and formation of focal adhesions [32]. The cells were then rinsed with PBS gently before adding CO_2-independent medium. The dish is then placed on the inverted microscope and a transfected cell that is attached to a single magnetic bead is located. Before mechanical stress application, the bead is magnetized in the horizontal direction for a very brief period (<100 μs) by a magnetic pulse. Cyan and Yellow fluorescence baseline images were collected before a vertical, homogeneous, constant magnetic field was subsequently applied to the bead to generate rotational forces on the bead. The Rac activity was visualized simultaneously by collecting dual simultaneous images of CFP and YPet of the cell on the same screen using the Dual View

system. Alternatively, PDGF was added to the cell-containing medium and Rac activity was quantified using the same method of FRET microscopy.

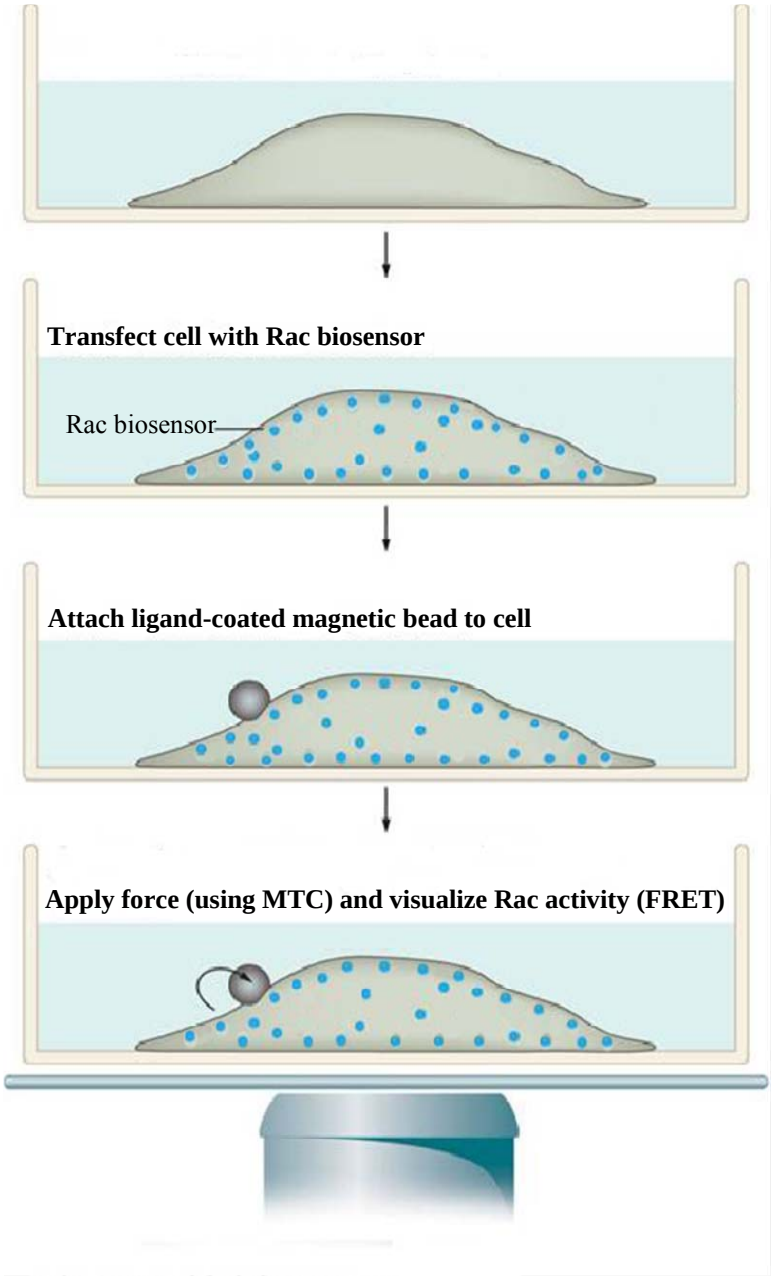

Figure 5. *Schematic of protocol. Live adherent cells are transfected using lipofectamine with the CFP-YFP Rac biosensor that binds to the plasma membrane. Twenty four hours after transfection, an RGD coated ferromagnetic bead is attached to the apical surface of*

the cell. The dish containing the cells is mounted on an inverted microscope to monitor Rac activity in response to stress application by magnetic bead twisting. (Modified from [28])

CHAPTER 3

RESULTS

3.1 Rac Activation by Stress and Growth Factor

We first determined how fast Rac could be activated by applied stress. As soon as the local mechanical stress (17.5 Pa, step function) was applied, the Rac GTPase was activated within 300 ms, as evidenced by the significant changes in FRET at the cell peripheries (Fig. 6A, C). It is interesting that the Rac activation occurs only at some sites on the cell surface (see insets in Fig. 6A). In contrast, the PDGF (10 ng/ml) induced Rac activation only occurred ~30 sec after the growth factor treatment (Fig. 6B, D). This suggests that force-induced Rac activation is much faster than growth factor induced signal transduction, consistent with the published results in Src activation [36]. To determine the specificity of the Rac biosensor, we transfected a mutant form of the biosensor RacN17 into the cells [31]. Neither stress nor PDGF activated the RacN17 biosensor, suggesting that the activation of Rac by stress or PDGF was specific to the Rac molecule.

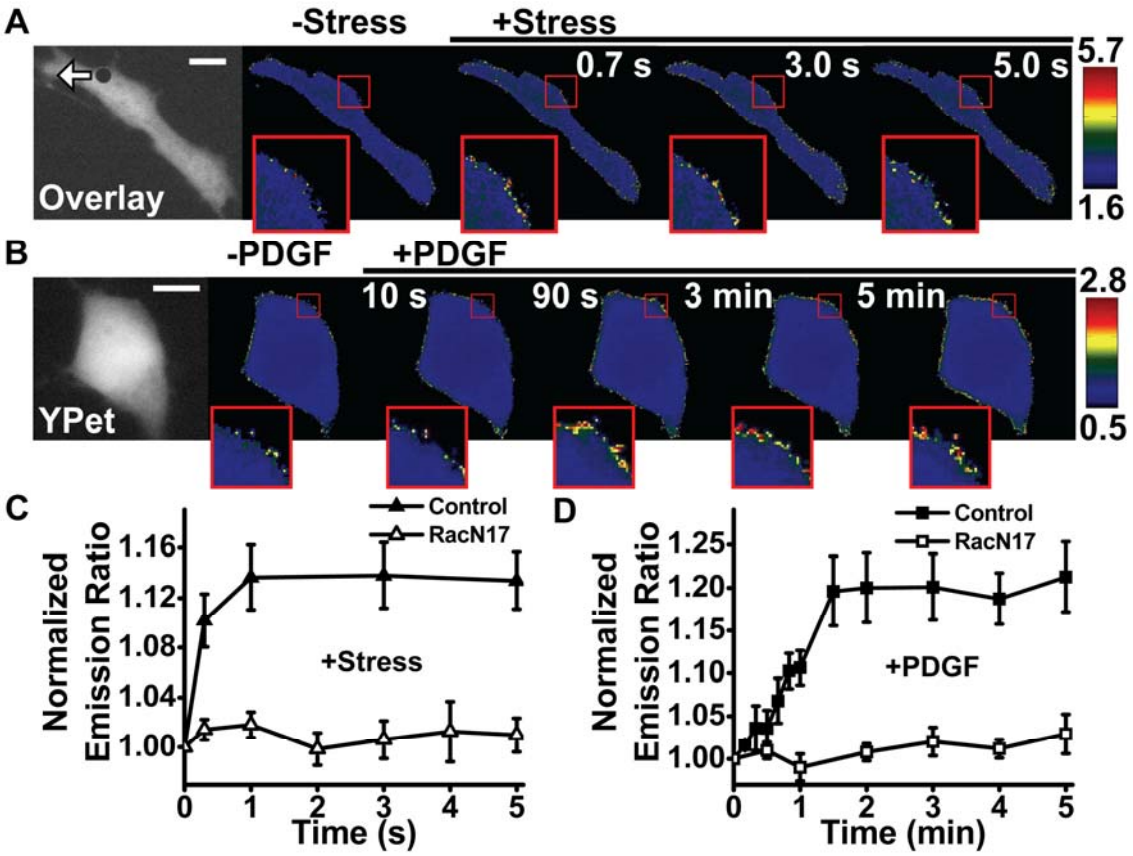

Figure 6. *Rapid Rac activation in response to a local mechanical stress. (A) A 4.5-μm RGD-coated ferromagnetic bead was attached to the apical surface of the cell (black dot is the bead) for 15 min to allow integrin clustering and formation of focal adhesions around the bead. The bead was magnetized horizontally and subjected to a vertical magnetic field (step function) which applies a mechanical rotational stress (apparent average stress=17.5 Pa) to the cell. A genetically encoded, CFP-YPet cytosolic Rac reporter was transfected into the smooth muscle cells following published procedures. The cytosolic Rac reporter was uniformly distributed in the cytoplasm (YPet fluorescence; white arrow indicates bead movement direction). The stress application induced rapid changes (<0.3 s) in FRET of the Rac reporter at discrete, distant sites at the cell periphery (the focal plane is ~1 μm above cell base), indicating rapid Rac activation (see Insets). Images are scaled and regions of large FRET changes (strong Rac activity) are shown in red/yellow. Scale bar = 10 μm. (B) Time-lapse images of Rac activation at the cell periphery after addition of PDGF (10 ng/ml) shows that activation*

of Rac in a representative cell by soluble factor PDGF is slow. Note that significant Rac activation occurred only at 0.5-1 min after PDGF treatment. Insets are enlarged areas showing Rac activation at the cell periphery. Scale bar = 10 μm. (C) Normalized emission ratio of FRET as a function of stress application duration for the Rac biosensor (control) and its mutant form(RacN17) (Control, n=6 cells; RacN17, n=3 cells; mean +/- s.e.). A representative cell was shown in A with the Rac biosensor. (D) Normalized YPet/CFP emission ratio time courses of the Rac biosensor (Control) and the mutant Rac biosensor (RacN17) in response to PDGF treatment. (Control, n=4 cells; RacN17, n=3 cells; mean +/- s.e.).

3.2 Stress-Induced Rac Activation Independent of Src

Since it has recently been shown that the PDGF-induced Rac activation is dependent on Src activation [26], we wondered whether the stress-induced Rac activation followed the same hierarchical signaling pathway. To determine this, we pretreated the cell with a specific Src inhibitor, PP1 (10 μM for 1 hr) before stress application. Surprisingly, there was no change in stress-induced Rac activation despite the fact that Src was inhibited (Fig. 7A, B, comparing to Fig. 6A, C). This result is drastically different from the PDGF-induced Rac activation which is blocked by Src inhibition with PP1 [26]. To further confirm our results from PP1-treated cells, we measured Rac activation in Src/Yes/Fyn triple-knockout (SYF-/-) mouse embryonic fibroblasts (MEFs). The same stress induced similar Rac activation at the cell periphery (Fig. 7C, D). These results are fundamentally different from the recent finding that the PDGF-induced Rac activation was inhibited in these SYF-/- MEFs [26]. The stress-induced Rac activation was specific for the integrin-cytoskeleton structural pathway, since the same magnitude of stress applied with magnetic beads coated with transferrin or poly-L-lysine failed to activate Rac (Fig. 7D).

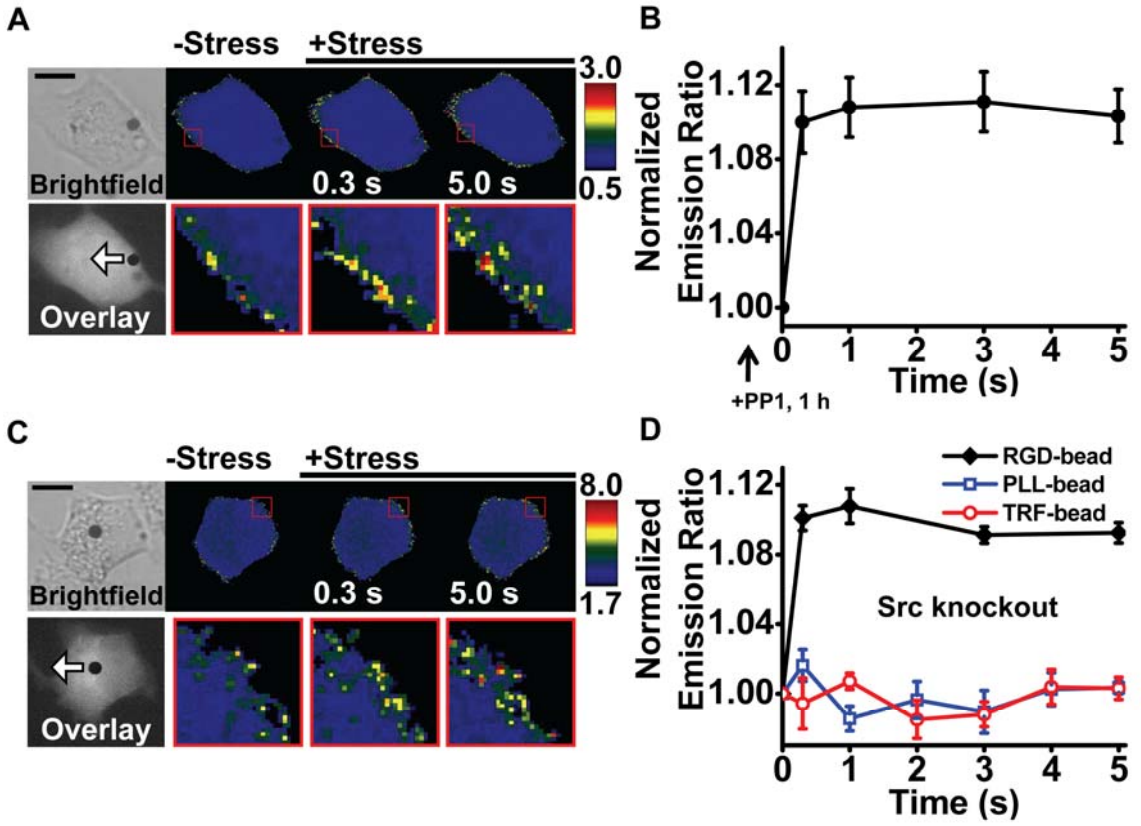

Figure 7. *Stress-induced Rac activation is independent of Src activity. (A) Time-lapse images of a representative smooth muscle cell transfected with the Rac biosensor and pretreated with a specific Src inhibitor, PP1 (10 μM for 1 hr), before stress application. Florescence resonance energy transfer (FRET) changes were observed within 0.3 s after stress application as shown in the inset with enlarged cell periphery. White arrow indicates magnetic bead movement direction when a stress of 17.5 Pa is applied. Scale bar = 10 μm. (B) Average data showing rapid Rac activation by stress even though Src was inhibited by PP1. (n=6 cells, mean +/- s.e.). (C) Time-lapse emission ratio images of the Rac biosensor in response to 17.5 Pa stress in a representative Src/Yes/Fyn triple-knockout (SYF-/-) MEF cell. The inset with the enlarged area of the cell periphery shows rapid activation of Rac. White arrow indicates RGD coated magnetic bead movement direction. Scale bar = 10 μm. (D) Probe specificity of Rac activation. Normalized YPet/CFP emission ratio shows that Rac activation is induced in SYF-/- mouse MEFs by mechanical stress applied via RGD-coated magnetic beads that bind specifically to*

integrin receptors (n=6 cells). Although the PDGF-induced Rac activation is known to be downstream of Src [26], knocking-out Src did not prevent Rac activation by stress. However, application of the same magnitude of stress at 17.5 Pa with beads coated with transferrin (TRF-bead) or poly-L-lysine (PLL-bead) did not activate Rac (TRF-bead, n=4 cells; PLL-bead, n=4 cells). Mean +/- s.e.

3.3 Effect of Lipid Rafts on Rac Activation by Stress

Since Rac localizes at the cell membrane [37], we decided to test if Rac activation depends on lipid rafts in the plasma membrane. We extracted cholesterol with methyl-beta-cyclodextrin (MβCD) (10 mM for 15 min) [38]. Interestingly, pretreatment of MβCD did not abolish activation of Rac by stress (Fig. 8). This result indicates that the stress-induced Rac activation is independent of lipid rafts at the plasma membrane.

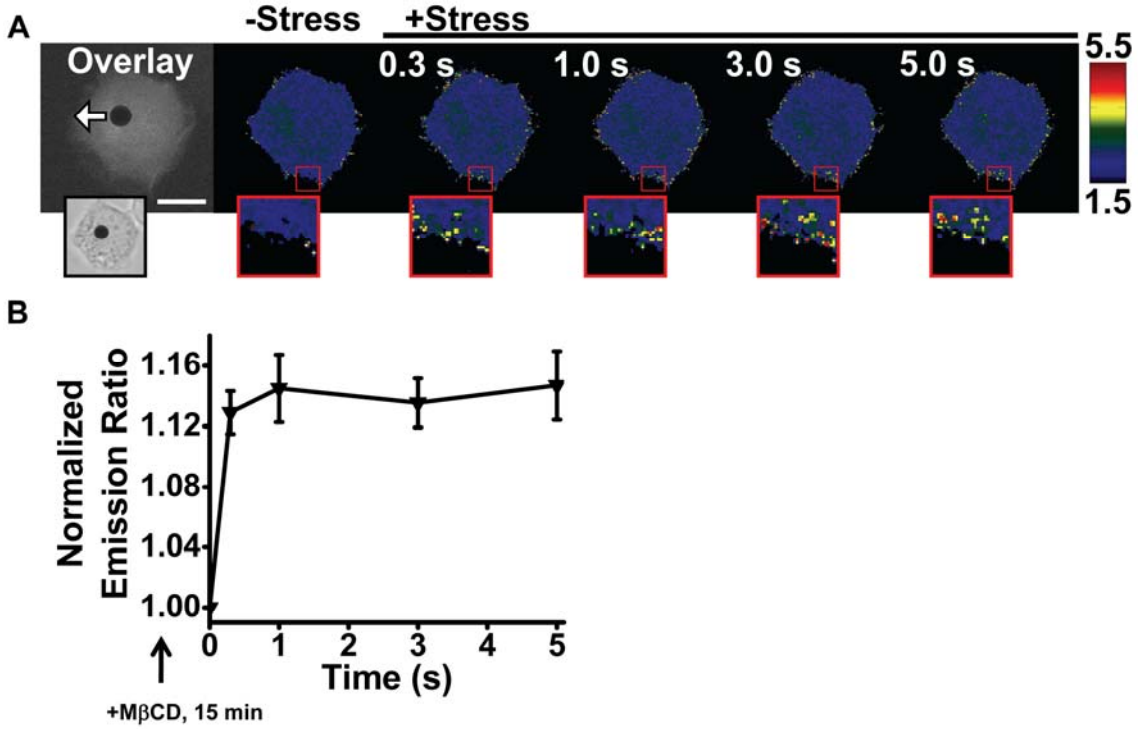

Figure 8. *Rapid Rac activation despite extraction of cholesterol from the plasma membrane. (A) Representative time-lapse emission ratio images of a SYF-/- MEF cell treated with 10 mM of methyl-β-cyclodextrin (MβCD) for 15 min to selectively extract cholesterol from the plasma membrane before the application of stress. Inset shows the enlarged area of the cell periphery where rapid activation of Rac is observed. The left inset panel shows the brightfield image of the cell with a magnetic bead (black dot) bound to the apical surface. (B) Normalized emission ratio time course of SYF -/- MEFs in response to 17.5 Pa stress pretreated with methyl-β-cyclodextrin (MβCD). This shows that the activation of Rac occurs independent of the integrity of lipid rafts at the plasma membrane. (n=4 cells, mean +/- s.e.)*

3.4 Specificity and Magnitude Dependence of Stress-Induced Rac Activation

To further test the specificity of the stress-induced Rac activation, we pretreated the cell with a known specific Rac inhibitor, NSC23766 (100 μM for 1 hr) [39].

Pretreatment with NSC23766 completely prevented the stress-induced Rac activation (Fig. 9). Together with the data with the mutant RacN17 biosensor in Fig. 6C, these results demonstrate that stress-induced Rac activation was not due to the unspecific conformational changes in the biosensor.

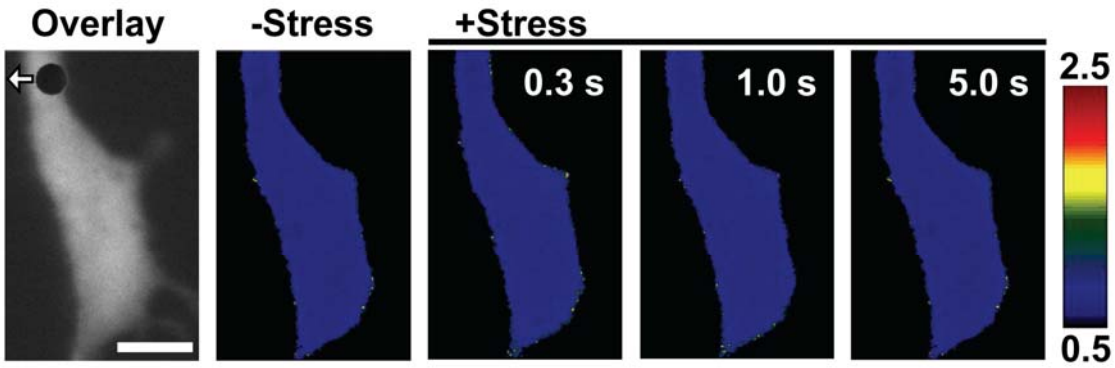

Figure 9. *Rac activation by stress is specific. The cell was pretreated with a specific Rac inhibitor, NSC23766 (25 μM for 1 hr) before stress application. The rest of the protocol was the same as in Fig. 6 (A). There were no changes in FRET ratios in response to stress, suggesting that the drug prevented stress-induced Rac activation. Two other cells showed similar behavior. Left panel shows the YPet fluorescent image of the cell with the magnetic bead overlaid on top. White arrow represents bead movement direction. Scale bar= 10 μm.*

If the Rac activation were directly induced by stress, it must depend on the magnitude of the applied stress. Indeed, our data showed that the stress threshold for Rac activation was between 8.8 and 17.5 Pa (Fig. 10). These results support the idea that Rac was rapidly activated by the stress applied via the magnetic bead bound to the integrin receptors.

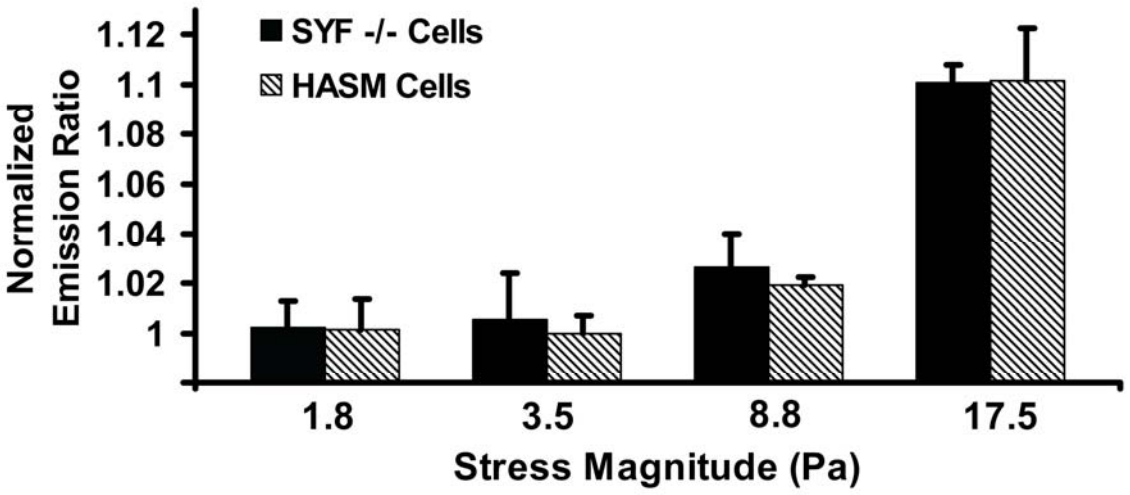

Figure 10. *Rac activation is dependent on the stress-magnitude. Bar graphs represent the normalized emission ratios of the YPet/CFP Rac biosensor in human airway smooth muscle (HASM) cells and SYF-/- MEFs at the time point of 0.3 s upon stress application. There were no significant differences in Rac activation between 1.8 and 3.5 Pa stress, or between 3.5 and 8.8 Pa stress ($p>0.05$), but there were significant differences between8.8 and 17.5 Pa stress ($p<0.01$), for either HASM or SYF-/- MEF cells. These data suggest that stress threshold for Rac activation is between 8.8 and 17.5 Pa. At 1.8 Pa, n=6 or 7; at 3.5 Pa, n=5 or 7; at 8.8 Pa, n=5 or 8; at 17.5 Pa, n=6; for HASM or SYF-/- MEFs, respectively. Mean +/- s.e.*

CHAPTER 4

DISCUSSION

The mechanism of mechanotransduction, i.e., how mechanical forces are converted into biochemical activities within the cell is a central question in cell biology. Our findings demonstrate that the plasma membrane bound Rac at remote sites or even at opposite ends of the local stress application site (i.e., the site of the bead) can be activated directly and rapidly. This finding clearly challenges the established dogma in the field of cell biology. Our results also challenge the established classical continuum mechanics theory of St. Venant's principle that a local force can only cause a local deformation. Our results are consistent with a recently published report that Src protein is directly activated by local mechanical stresses [36] and action at a distance in living cells [40, 41]. However, there are differences between our study and the study done by Na *et al*. Src is a protein that localizes on the endosomal membranes, which in turn are connected with microtubules. Thus Src is directly activated via microtubule deformation [36]. In contrast, Rac is a plasma membrane bound protein. It is well known that the plasma membrane is rather fluid and thus dissipate forces very rapidly. Therefore, it is not clear how the plasma membrane-bound Rac is activated by a local force. An additional piece of evidence for the difference between Src and Rac is that the threshold stress for Rac activation is ~5-fold higher than for Src activation (~10 Pa for Rac, 1.8 Pa for Src) in the same human airway smooth muscle cell (Fig. 10; ref. 36). It is interesting that two different types of cells (fibroblasts and smooth muscle cells) exhibit similar threshold stresses for Rac activation, suggesting that the setpoint for the enzyme activation is the

threshold strain (deformation), since both cell types have similar softness (or its inverse, stiffness). This interpretation is consistent with our recent findings in embryonic stem cells and differentiated cells that cell softness dictates biological responses of a living cell to a local stress [42].

We wondered if Rac activation can be triggered by diffusion or translocation of molecules. It is known that calcium is one of the fastest diffusive molecules in the cytoplasm with a diffusion coefficient of ~60 $\mu m^2/s$ [43]. If calcium ion channels were opened as a result of the local mechanical force, then for a distance of 30 μm in the cytoplasm, it would take ~4 s [t=square of distance divided by four times diffusion coefficient=$(30\ \mu m)^2/[4x60\ \mu m^2/s]$=3.75 s] for calcium to reach Rac at the remote site. However, we observed that Rac activation occurs in less than 300 ms after force application. Therefore the activation speed is too rapid to be explained by calcium diffusion. Another possibility is protein translocation along the cytoskeleton to activate Rac. It is known that translocation speed is <4 μm/s in the cytoplasm [44]. Hence it would take at least 7 s for the protein to be translocated across a distance of 30 μm. Again, this is too slow to explain the rapid activation of Rac that we have observed in living cells.

Alternatively, it is possible that a local force applied to integrin receptors propagates along the tensed actin bundles and reach remote sites in the cytoplasm within 1 ms through elastic wave propagation without significant decreasing in stress magnitudes [36], which in turn leads to a deformation of cytoskeleton filaments such as microfilaments, microtubules and intermediate filaments [45]. This model of the integrin-cytoskeleton force transduction pathway is supported by the data that inhibiting

myosin-II dependent tension with blebbistatin, disrupting F-actin with cytochalasin D, or disrupting microtubules with colchicine, all blocked stress-induced Rac activation (Fig. 11A, B). Some of these cytoskeletal networks may form strong connections with the plasma membrane at certain sites. It is at these sites that Rac GTPase is activated. A working model for force-induced rapid Rac activation is illustrated in Fig. 12.

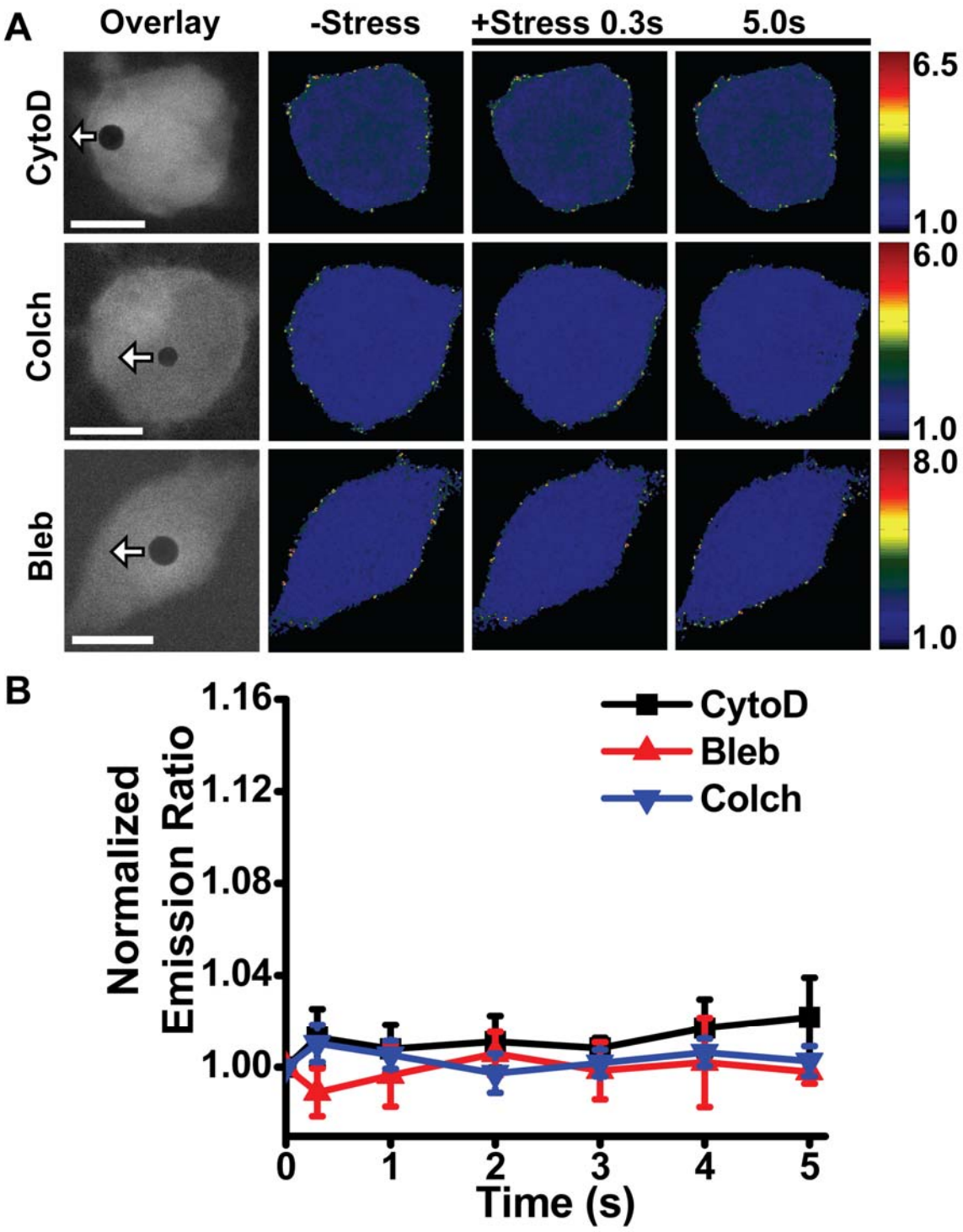

Figure 11. *Cytosketal integrity is necessary for Rac activation by stress. (A) Mechanical stimulation of Src/Yes/Fyn triple-knockout (SYF -/-) MEF cells pretreated with different specific cytoskeletal disrupting drugs did not induce Rac activation. Cells were pretreated with Cytochalasin D (1 μg/ml for 15 min); Colchicine (10 μM for 15 min);*

and Blebbistatin (50 μM for 20 min). A RGD-coated magnetic bead was then bound to the cell for 15 min, followed by mechanical stress application of 17.5 Pa. White arrow indicates direction of magnetic bead movement. Scale bar = 10 μm. (B) Normalized YPet/CFP emission ratio over time shows that inhibition cytoskeletal tension with blebbistatin (Blebb, 50 μM for 30 min, n=7 cells), disrupting F-actin with cytochalasin D (CytoD, 1 μg/ml for 15 min, n=6 cells) or microtubules with colchicines (Colch, 10 μM for 15 min, n=9 cells), prevented stress-induced Rac activation in SYF-/- MEFs (mean +/- s.e.). Representative cell for each condition is shown in A.

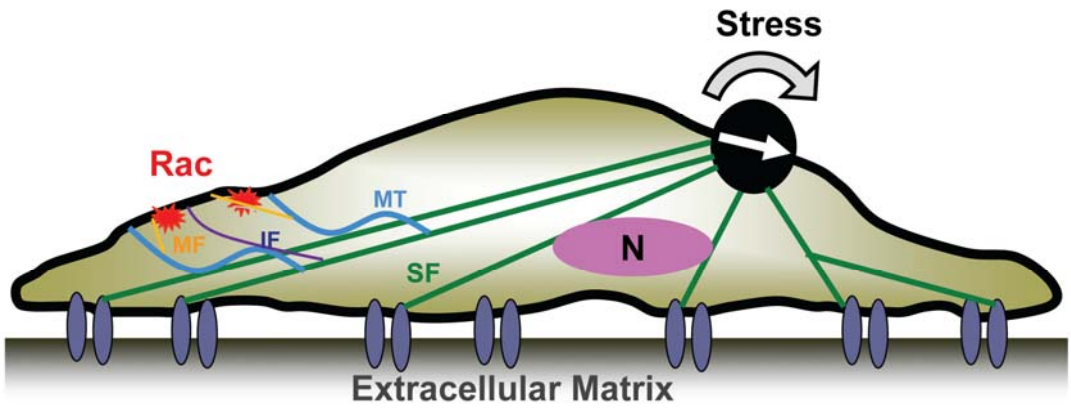

Figure 12. *A working model for rapid Rac activation by stress. A local load (magnetic bead) applied to focal adhesions leads to stress propagation along the actin bundles (red lines) without decay in magnitudes at remote sites. Rac GTPase bound to the plasma membrane at the other end of the cell are activated rapidly when stress waves reach the plasma membrane via the cytoskeleton to directly deform Rac, causing a conformational change in the enzyme. MF= actin microfilament; MT=microtubule; IF=intermediate filament; SF=stress fiber; N=nucleus (not drawn to scale). Black dot=the magnetic bead. White arrow=magnetic moment direction of the magnetized bead. Curved black arrow=the rotational shear stress.*

It is known that uniaxially stretching a whole cell by a flexible substrate increases Rac activation, possibly by tension, whereas at the lateral sites Rac activity is inhibited, possibly by compression [46]. Since we apply a rotational shear stress to the cell surface via the magnetic bead, it is possible that the Rac activation sites in our cells are the sites where local tension is increased. This possibility needs to be tested in future studies.

Future work is also needed to determine the role of substrate stiffness in regulating the stress-induced Rac activation [47]. Furthermore, to test our working model for the stress-induced direct Rac activation, the structural basis for Rac activation needs to be elucidated to find out which cytoskeletal filament systems are the most important in mediating the propagation of stresses to activate Rac. In addition to Src, it is shown that phosphatidylinositol-3-kinase (PIP3 kinase) can facilitate recruitment of Rac to cell membrane [48]. Since Rac and Rho proteins are negative regulators of each other [49], it remains to be seen if the stress-induced Rac activation leads to inhibition of Rho at the cell periphery.

Mechanochemical conversion like what we have demonstrated in this study occurs in cells, tissues, and organs as forces are transmitted over load bearing networks like bones, muscles, extracellular matrix, integrins, cell-cell junctions, cytoskeletal filaments and nuclear scaffolds [1]. The cells sense these forces exerted on tissues and organs through their interconnections with the extracellular matrix which transduces in to biochemical activity [1]. There is ample evidence that mechanical and chemical stimulation play critical roles in determining cell properties, like morphology, cell fate, and gene transcription. However, despite the remarkable progress, there is still no formulation of physical laws from which we may predict cell motion, stem cell fate, or

the shape cell assumes [50]. Eventually, one would like to know how soluble factor stimulation integrates with mechanical stimuli in a living cell to produce a cohesive biological response such as gene expression.

CHAPTER 5
CONCLUSION

In summary, we have found that a local stress of physiologic magnitude can directly activate Rac GTPase rapidly, independent of the Src activity. In contrast to the theory of classical continuum mechanics of St. Venant's principle, as well as previously proposed mechanotransduction models that require diffusion or translocation of biochemical signaling molecules, we show that mechanical force at the plasma membrane can be transmitted through the cytoskeleton to deep remote cytoplasmic sites [40 , 51] inducing conformational changes of proteins that are physically linked to the cytoskeleton [36]. The observed mechanical stress induced signal transduction occurs too rapidly (<0.3 s) to be explained by the diffusion or translocation mechanism. Therefore, we a different model of stress-wave propagation along cytoskeletal filaments is used to explain our observations. In principle our approach of combining FRET with a local stress application can be extended to any molecules in a living cell [52]. Our finding on the stress-induced rapid Rac activation challenges the conventional wisdom on mechanotransduction and suggests that stress-induced signaling does not follow signal transduction pathways induced by growth factors. However, it remains to be seen how stress induced rapid Rac activation may influence cell division, motility, adaptation and remodeling.

REFERENCES

1. Ingber DE (2006) Cellular mechanotransduction: putting all the pieces together again. FASEB J. 20: 811-827.

2. Ingber DE (2003) Tensegrity II. How structural networks influence cellular information processing networks. J. Cell Sci. 116: 1397-1408.

3. Matthews BD, Overby DR , Mannix R, Ingber DE (2006) Cellular adaptation to mechanical stress: role of integrins, Rho, cytoskeletal tension and mechanosensitive ion channels. J. Cell Sci. 119: 508-18.

4. Leckband D, Prakasam A (2006) Mechanism and Dynamics of Cadherin Adhesion. Annu Rev Biomed Eng 8: 259-287.

5. Hahn C, Schwartz MA (2009) Mechanotransduction in vascular physiology and atherogenesis. Nat Rev Mol Cell Biol 10(1):53-62

6. Huang S, and Ingber DE (1999) The structural and mechanical complexity of cell-growth control. Nat Cell Biol 1(5):E131–E138

7. Engler AJ, Sen S, Sweeney HL, and Discher DE. (2006) Matrix elasticity directs stem cell lineage specification. Cell 126(4):677–689, 2006.

8. Vogel V, Sheetz M (2006) Local force and geometry sensing regulate cell functions. Nat. Rev. Mol. Cell Biol. 7: 265-275.

9. Pelham RJ Jr, Wang YL (1997) Cell locomotion and focal adhesions are regulated by substrate flexibility. Proc Natl Acad Sci USA 94:13661–13665.

10. Giannone G, Dubin-Thaler BJ, Dobereiber HG, Kieffer N, Bresnick AR, et al (2004) Periodic lamellipodial contractions correlate with rearward actin waves. Cell 116:431–443

11. Wang Y, Chang J, Chen KD, Li S, Li J, et al. (2007) Selective adapter recruitment and differential signaling networks by VEGF vs. shear stress. Proc Natl Acad Sci USA 104:8875–8879

12. Lele TP, Pendse J, Kumar S, Salanga M, Karavitis J, et al. (2006) Mechanical forces alter zyxin unbinding kinetics within focal adhesions of living cells. J Cell Physiol 207:187–194

13. Riveline D, Zamir E, Balaban NQ, Schwarz US, Ishizaki T**,** et al. (2001) Focal contacts as mechanosensors: Externally applied local mechanical force induces growth of focal contacts by an mDia1-dependent and ROCK-independent mechanism. J Cell Biol 153:1175–1186

14. Trepat X, Deng L, An SS, Navajas D, Tschumperlin DJ, et at. (2007) Universal physical responses to stretch in the living cell. Nature 447:592–595

15. Mitra SK, Schlaepfer DD (2006) Integrin-regulated FAK-Src signaling in normal and cancer cells. Curr Opin Cell Biol 18:516-23

16. Eliceiri BP, Paul R, Schwartzberg PL, Hood JD, Leng J, et al. (1999) Selective requirement for Src kinases during VEGF-induced angiogenesis and vascular permeability. Mol Cell 4:915-24.

17. Felsenfeld DP, Schwartzberg PL, Venegas A, Tse R, Sheetz MP. (1999) Selective regulation of integrin--cytoskeleton interactions by the tyrosine kinase Src. Nat Cell Biol. 1:200-6

18. Critchley DR. (2000) Focal adhesions - the cytoskeletal connection. Curr Opin Cell Biol. 12:133-9

19. Chicurel ME, Singer RH, Meyer CJ, Ingber DE. (1998) Integrin binding and mechanical tension induce movement of mRNA and ribosomes to focal adhesions. Nature. 392:730-3.

20. Jiang G, Kennedy MJ, Christie-Blick N. (2003) Stable isotopic evidence for methane seeps in Neoproterozoic postglacial cap carbonates. Nature 426:822-6.

21. Arias-Salgado EG, Lizano S, Sarkar S, Brugge JS, Ginsberg MH, et al. (2003) Src kinase activation by direct interaction with the integrin beta cytoplasmic domain. Proc Natl Acad Sci U S A. 100:13298-302

22. Hall A. (2005) Rho GTPases and the control of cell behaviour. Biochem Soc Trans. 33:891-5

23. Ridley AJ, Hall A. (1992) The small GTP-binding protein rho regulates the assembly of focal adhesions and actin stress fibers in response to growth factors. Cell 70:389-99

24. Ridley AJ, Paterson HF, Johnston CL, Diekmann D, Hall A. (1992) The small GTP-binding protein rac regulates growth factor-induced membrane ruffling. Cell 70:401-10

25. Wang Y, Botvinick EL, Zhao Y, Berns MW, Usami S, et al. (2005) Visualizing the mechanical activation of Src. Nature 434: 1040-1045.

26. Ouyang M, Sun J, Chien S , Wang Y (2008) Determination of hierarchical relationship of Src and Rac at subcellular locations with FRET biosensors. Proc. Natl. Acad. Sci. USA. 105: 14353-14358.

27. Troung K, Ikura M (2001) The use of FRET imaging microscopy to detect protein-protein interactions and protein conformational changes in vivo. Curr Opin Struct Biol 11:573-578

28. Na S , Wang N (2008) Application of Fluorescence Resonance Energy Transfer and Magnetic Twisting Cytometry to Quantify Mechano-Chemical Signaling Activities in a Living Cell. Science Signaling 1: pl1.

29. Panettieri RA, Murray RK, DePalo LR, Yadvish PA , Kotlikoff MI (1989) A human airway smooth muscle cell line that retains physiological responsiveness. Am. J. Physiol. Cell Physiol. 25: C329-C335.

30. Itoh RE, Kurokawa K, Ohba Y, Yoshizaki H, Mochizuki N, et al. (2002) Activation of rac and cdc42 video imaged by fluorescent resonance energy transfer-based single-molecule probes in the membrane of living cells. Mol. Cell Biol. 22: 6582-6591.

31. Wang N, Ingber DE. (1995) Probing transmembrane mechanical coupling and cytomechanics using magnetic twisting cytometry. Biochem. Cell Biol. 73: 327-335.

32. Wang N, Butler JP, Ingber DE (1993) Mechanotransduction across the cell surface and through the cytoskeleton. Science 260: 1124-1127.

33. Fabry B, Maksym GM, Shore SA, Moore PE, Panettieri RA, et al. (2001) Time course and heterogeneity of contractile responses in cultured human airway smooth muscle cells. J. Appl. Physiol. 91: 986-994.

34. Valberg PA, Butler JP (1987) Magnetic particle motions within living cells. Biophys J. 52:537-550

35. Otsu N. (1979) A threshold selection method for gray-level histograms. IEEE Trans. Syst. Man Cybern 9:62-66

36. Na S, Collin O, Chowdhury F, Tay B, Ouyang M, et al. (2008) Rapid signal transduction in living cells is a unique feature of mechanotransduction. Proc. Natl. Acad. Sci. USA 105: 6626-6631.

37. Moissoglu K, Slepchenko BM, Meller N, Horwitz AF, Schwartz MA (2006) In Vivo Dynamics of Rac-Membrane Interactions. Mol. Biol. Cell 17: 2770–2779.

38. Rodal SK, Skretting G, Garred O, Vilhardt F, van Deurs B, et al. (1999) Extraction of cholesterol with methyl-beta-cyclodextrin perturbs formation of clathrin-coated endocytic vesicles. Mol. Biol. Cell. 10: 961-74.

39. Gao Y, Dickerson JB, Guo F, Zheng J, Zheng Y (2004) Rational design and characterization of a Rac GTPase-specific small molecule inhibitor. Proc. Natl. Acad. Sci. U S A. 101: 7618-23.

40. Hu S, Chen J, Fabry B, Numaguchi Y, Gouldstone A, et al. (2003) Intracellular stress tomography reveals stress focusing and structural anisotropy in the cytoskeleton of living cells. Am. J. Physiol. Cell Physiol. 285: C1082-C1090.

41. Hu S, Eberhard L, Chen J, Love JC, Butler JP, et al. (2006) Mechanical anisotropy of adherent cells probed by a three dimensional magnetic twisting device. Am. J. Physiol. Cell 287: C1184-C1191.

42. Chowdhury F, Na S, Li D, Poh YC, Tanake T, et al. (2009) Material properties of the cell dictate stress-induced spreading and differentiation in embryonic stem cells. Nat. Materials. DOI: 10.1038/NMAT2563.

43. Hayakawa K, Tatsumi H , Sokabe M (2008) Actin stress fibers transmit and focus force to activate mechanosensitive channels. J. Cell Sci. 121: 496-503.

44. Kural C, Kim H, Syed S, Goshima G, Gelfand VI , et al. (2005). Kinesin and dynein move a peroxisome in vivo: a tug-of-war or coordinated movement? Science 308: 1469-1472.

45. Eckes B, Dogic D, Colucci-Guyon E, Wang N, Maniotis A, et al. (1998) Impaired mechanical stability, migration, and contractile capacity in vimentin-deficient fibroblasts. J. Cell Sci. 111: 1897-1907.

46. Katsumi A, Milanini J, Kiosses WB, del Pozo MA, Kaunas R, et al. (2002) Effects of cell tension on the small GTPase Rac. J. Cell Biol. 158: 153-64.

47. Discher DE, Janmey P, Wang YL (2005) Tissue cells feel and respond to the stiffness of their substrate. Science 310: 1139-43.

48. Bäumer AT, ten Freyhaus H, Sauer H, Wartenberg M, Kappert K, et al. (2008) Phosphatidylinositol 3-Kinase-dependent Membrane Recruitment of Rac-1 and p47phox Is Critical for-Platelet-derived Growth Factor Receptor-induced Production of Reactive Oxygen Species. J. Biol. Chem. 283:7864–7876

49. Pertz O, Hodgson L, Klemke RL , Hahn KM (2006) Spatiotemporal dynamics of RhoA activity in migrating cells. Nature 440: 1069-72.

50. Haw M. (2007) From steam engines to life. Am. Sci. 95:472–473.

51. Wang N, Suo Z. (2005) Long-distance Propagation of Forces in a Cell. Biochem Biophys Res Commun, 328:1133-1138

52. Wang Y, Wang N (2009) FRET and mechanobiology. Integrative Biol. 1: 565-573.

AUTHOR'S BIOGRAPHY

Yeh Chuin Poh was born in Kuala Lumpur, Malaysia on December 30th, 1986. He obtained his B.S.E degree in Mechanical Engineering from the University of Michigan, Ann Arbor. His interest in mechanobiology escalated after being given the opportunity to be a research assistant under the guidance of Professor Ning Wang. Upon graduation, Yeh Chuin hopes to pursue a PhD degree in the same field. Yeh Chuin has thus far co-authored three scientific journal papers.